Cancer Research

Frequent *PVT1* Rearrangement and Novel Chimeric Genes *PVT1-NBEA* and *PVT1-WWOX* Occur in Multiple Myeloma with 8q24 Abnormality

Hisao Nagoshi[1,2], Tomohiko Taki[2], Ichiro Hanamura[3], Masakazu Nitta[3], Takemi Otsuki[4], Kazuhiro Nishida[1], Keiko Okuda[2], Natsumi Sakamoto[1], Satoru Kobayashi[1], Mio Yamamoto-Sugitani[1], Yasuhiko Tsutsumi[1], Tsutomu Kobayashi[1], Yosuke Matsumoto[1], Shigeo Horiike[1], Junya Kuroda[1], and Masafumi Taniwaki[1,2]

Abstract

Chromosome 8q24 rearrangements are occasionally found in multiple myeloma and are associated with tumor progression. The 8q24 rearrangements were detected by FISH in 12 of 54 patients with multiple myeloma (22.2%) and in 8 of 11 multiple myeloma cell lines (72.7%). The breakpoints of 8q24 in 10 patients with multiple myeloma and in all multiple myeloma cell lines were assigned to a 360 kb segment, which was divided into 4 regions: approximately 120 kb centromeric to *MYC* (5′ side of *MYC*), the region centromerically adjacent to *PVT1* (∼ 170 kb region, including *MYC*, of 5′ side of *PVT1*), the *PVT1* region, and the telomeric region to *PVT1*. *PVT1* rearrangements were most common and found in 7 of 12 patients (58.3%) and 5 of 8 cell lines (62.5%) with 8q24 abnormalities. A combination of spectral karyotyping (SKY), FISH, and oligonucleotide array identified several partner loci of *PVT1* rearrangements, such as 4p16, 4q13, 13q13, 14q32, and 16q23-24. Two novel chimeric genes were identified: *PVT1-NBEA* in the AMU-MM1 cell line harboring t(8;13)(q24;q13) and *PVT1-WWOX* in RPMI8226 cell line harboring der(16)t(16;22)ins(16;8)(q23;q24). The *PVT1-NBEA* chimera in which *PVT1* exon 1 was fused to *NBEA* exon 2 and the *PVT1-WWOX* in which *PVT1* exon 1 was fused to *WWOX* exon 9 were associated with the expression of abnormal *NBEA* and *WWOX* lacking their N-terminus, respectively. These findings suggest that *PVT1* rearrangements may represent a novel molecular paradigm underlying the pathology of 8q24 rearrangement–positive multiple myeloma. *Cancer Res; 72(19); 4954–62. ©2012 AACR.*

Introduction

Genetic abnormalities play a crucial role in the pathogenesis of various malignancies, including multiple myeloma. The primary cytogenetic abnormalities associated with disease development are either nonrandom chromosomal gains known as hyperdiploid, which is characterized by trisomies of chromosomes 3, 5, 7, 9, 11, 15, 19, and 21, or structural rearrangements involving the immunoglobulin heavy chain gene (*IGH*) located at 14q32.33 (*IGH* translocation; refs. 1, 2). Secondary cytogenetic abnormalities implicated in disease progression include 8q24 rearrangements, gain of the long arm of chromosome 1 (1q+), and loss of the short arm of chromosome 17 (17p; refs. 1, 3).

The 8q24 rearrangements have been identified by conventional cytogenetic analysis in 3.5% to 5.0% of patients with multiple myeloma (4, 5), and by FISH and spectral karyotyping (SKY) in 9.5% to 20% (6–9). The 8q24 rearrangements are frequently associated with advanced disease in patients with multiple myeloma and multiple myeloma cell lines (10, 11). Ig chromosomal translocations, such as t(8;14)(q24;q32) and t(8;22)(q24;q11), occur in approximately 25% of multiple myelomas with 8q24 rearrangements, whereas non-Ig chromosomal loci, including 1p13, 1p21-22, 6p21, 6q12-15, 13q14, and 16q22, in which no candidate genes have been delineated so far, have also been identified as translocation partners (7, 8, 12, 13). *MYC* has long been a possible candidate target gene for 8q24 rearrangements; however, many of the breakpoints within 8q24 have been assigned to various regions that encompassed more than 2 Mb centromeric or telomeric to *MYC* (9, 11). In contrast to the typical Burkitt lymphoma translocation t(8;14) with breakpoints within the *MYC* gene (14), rearrangements of *plasmacytoma variant translocation 1/Moloney leukemia virus integration-1 locus* (*PVT1*), which is located 57 kb 3′ of *MYC*, have been identified in variant Burkitt lymphoma translocations t(8;22) and t(2;8). In the latter

Authors' Affiliations: Departments of [1]Hematology and Oncology and [2]Molecular Diagnostics and Therapeutics, Kyoto Prefectural University of Medicine Graduate School of Medical Science, Kyoto; [3]Division of Hematology, Department of Internal Medicine, Aichi Medical University, Nagakute, Aichi; and [4]Department of Hygiene, Kawasaki Medical School, Kurashiki, Japan

Note: Supplementary data for this article are available at Cancer Research Online (http://cancerres.aacrjournals.org/).

Corresponding Author: Masafumi Taniwaki, Department of Hematology and Oncology, Kyoto Prefectural University of Medicine Graduate School of Medical Science, 465 Kajii-cho, Kawaramachi-Hirokoji, Kamigyo-ku, Kyoto 602-8566, Japan. Phone: 81-75-251-5740; Fax: 81-75-251-5743; E-mail: taniwaki@koto.kpu-m.ac.jp

doi: 10.1158/0008-5472.CAN-12-0213

translocations, fusion of the constant region of the *IG* γ or κ chain gene to *PVT1* was detected, resulting in a lack of protein production (15).

In this study, the 8q24 rearrangements were analyzed in patients with multiple myeloma and cell lines by FISH and SKY combined with oligonucleotide arrays. Results showed frequent *PVT1* rearrangements with several partners and novel *PVT1-NBEA* and *PVT1-WWOX* chimeric genes.

Materials and Methods

Patients and cell lines

The use of clinical samples was approved by the Institutional Review Board of Kyoto Prefectural University of Medicine (Kyoto, Japan). Informed consent was obtained from all patients. Primary samples were obtained from the bone marrow of 53 patients and the lymph node of 1 patient between April 2005 and January 2011. Eleven multiple myeloma cell lines, AMU-MM1, KMS-12-BM, KMS-18, KMS-20, KMS-28-PE, KMS-34, AMO1, IM9, LP-1, NCI-H929, and RPMI8226, were also analyzed. AMU-MM1 was established at Aichi Medical University (Aichi, Japan) from the tumor cells of the cerebrospinal fluid of a 72-year-old Japanese female patient with IgA-κ multiple myeloma (16).

FISH analysis

The FISH was conducted as described previously (17). To assess the 8q24 rearrangement patterns and identify the genes involved, 3 sets of probes were used. The first set of probes was the 8q24 probe-LSI MYC Dual Color, Break Apart Rearrangement Probe. It consists of the SpectrumOrange-labeled 5′ LSI *MYC* probe, which begins at 119 kb upstream of the 5′ end of *MYC* and extends 266 kb toward the centromere, and the SpectrumGreen–labeled 3′ LSI *MYC* probe, which starts approximately at 1.5 Mb 3′ of *MYC* and extends 407 kb toward the telomere (Abbott Japan). The second set of probes was designed to hybridize to both adjacent sides on the *PVT1* gene, defined as PVT1-adjacent (PVT1-A) probe. The PVT1-A probe set was composed of 2 specific bacterial artificial chromosome clones CTD-3066D1, a fragment approximately 170 kb in length adjacent to the 5′ end of *PVT1*, and RP11-628C14, a fragment approximately 190 kb in length adjacent to the 3′ end of *PVT1*. The third set of probes was the PVT1-spanning (PVT1-S) probe consisting of 2 bacterial artificial chromosome clones, CTD-22267H2, a fragment approximately 120 kb in length covering 5′ regions of *PVT1*, and RP11-164J24, a fragment approximately 190 kb in length covering 3′ regions of *PVT1* (Fig. 1A). For interphase analysis, signals were evaluated in a minimum of 100 nuclei with hybridization efficiency greater than 90%.

SKY analysis and SKY combined with FISH analysis

The SKY analysis was conducted as described previously (18). For the SKY–FISH analysis, SKY and FISH probe mixtures simultaneously hybridized to chromosomes for 2 days at 37°C. Ten to 20 metaphase spreads were analyzed, and karyotypes were defined according to ISCN 2009 (19). For complex abnormalities with rearranged 8q24 locus, such as translocations or insertions, which cannot be detected by either FISH or SKY, a SKY–FISH procedure was used to detect chromosomal locations involving *MYC* and *PVT1*.

Genome copy number analysis

The DNA gain and loss assay on the basis of high-density oligonucleotide microarrays (GeneChip Human Mapping 50K, 250K, or 6.0 single-nucleotide polymorphism (SNP) array, Affymetrix) was conducted with genomic DNA extracted from cell lines and tumor specimens. Breakpoints in chromosomal translocations were identified by the means of genome copy number analysis combined with SKY, and the SNP array data were analyzed to determine total copy numbers using the CNAG3.0 or 3.3 programs (20).

Reverse-transcription PCR and sequencing analysis

Reverse-transcription PCR (RT-PCR) analysis was conducted as described previously (21). The following primers were used: P1S (forward primer in exon 1 of *PVT1*, NR_003367.1), 5′-TTGCGGAAAGGATGTTGGCG-3′, and N3A (reverse primer in exon 3 of *NBEA*, NM_015678.3), 5′-GCTCCATATTTCTGCTTGACA-3′, for the detection of any chimeric gene on der(8)t(8;13); N2S (forward primer in exon 2 of *NBEA*), 5′-CATACAGGTCGGAGAGGTC-3′, and P2A (reverse primer in exon 2 of *PVT1*), 5′-AGGGCTTCACCGGCTCAAT-3′, or P3A (reverse primer in exon 3 of *PVT1*), 5′-GGGTCTTACATTCCATAGGG-3′, for the detection of any chimeric gene on der(13)t(8;13); and P1S and W9A (reverse primer in exon 9 of *WWOX*, NM_016373.2), 5′-CAGGGAGATACGGAACCTAC-3′, for the detection of any chimeric gene on der(16)t(16;22)ins(16;8)(q23;q24). The nucleotide sequences of PCR products were determined with the fluorometric method (Dye Terminator Cycle Sequencing Kit, Applied Biosystems).

Real-time quantitative RT-PCR

NBEA and *WWOX* mRNA levels were measured with specific primer probe sets from Assays-on-Demand (Applied Biosystems) or SYBR Green method using the ABI Prism 7300 system (Applied Biosystems) according to the manufacturer's instructions. Primers were Assays-on-Demand NBEA 2-3 (Hs00995629_m1), NBEA 58-59 (Hs00995655_m1), W8S (forward primer in exon 8 of *WWOX*), 5′-GCAACATCCTCTTCTCCAACGA-3′, WPA2(reverse primer in exon 9 of *WWOX*), 5′-TGGGACAGCAGCACAGTACA-3′, W9S (forward primer in exon 9 of *WWOX*), 5′-TGTACTGTGCTGCTGTCCCA-3′, and WPA3(reverse primer in exon 9 of *WWOX*), 5′-CCGTTCTTGGATCAGCCTC-3′. These primer sets were used to distinguish abnormal chimeric *NBEA* or *WWOX* transcripts from normal transcripts: NBEA 2-3, spanning the breakpoint of 8q24 in t(8;13)(q24;q14), can detect only the normal *NBEA* transcript, whereas NBEA 58-59 can detect both normal and chimeric transcripts, similarly, combination of W8S and W9A(2) can detect only the normal *WWOX* transcript and W9S and W9A(3) can detect both normal and chimeric *WWOX* transcripts. The *β-actin* mRNA level was measured as an internal control. In addition to the 11 multiple myeloma cell lines, normal peripheral lymphocytes, an Epstein–Barr virus–transformed B-cell line derived from a normal healthy volunteer, the erythroleukemia cell line K562, and the Burkitt

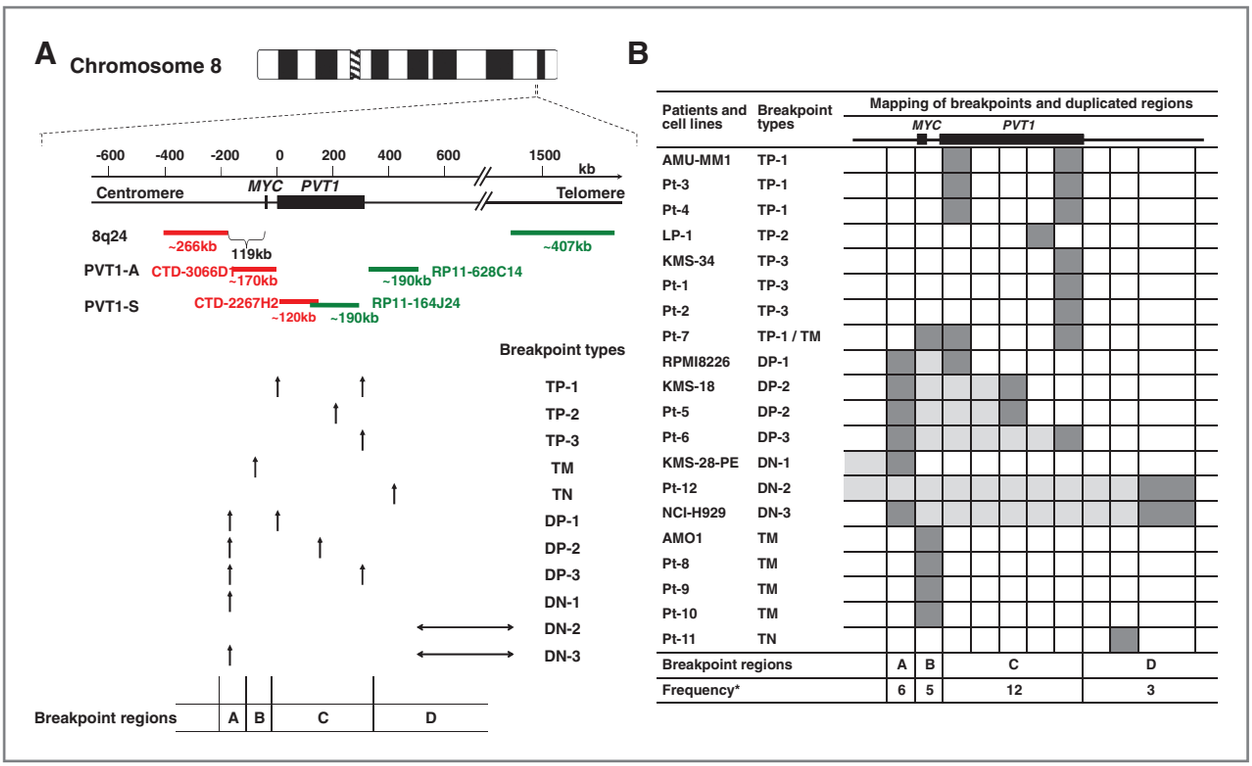

Figure 1. Identification of breakpoints region at 8q24 by FISH analysis. A, location of FISH probes and mapping of putative breakpoints at 8q24. FISH probes are depicted as color bars. Vertical arrows indicate breakpoints and horizontal double-headed arrows indicate the possible range of breakpoints on the basis of interphase FISH analysis. The combination of the FISH analysis with 3 sets of probes reveals 4 breakpoint regions and 11 breakpoint types as shown in B and Supplementary Fig. S1. B, mapping of breakpoints in patients with multiple myeloma and cell lines with 8q24 rearrangement. Dark gray boxes, the breakpoint regions; light gray boxes, duplicated regions. Pt, patient number. Breakpoint region A is the 120 kb length region of centromeric to *MYC*, B is the 170 kb length region centromerically adjacent to *PVT1* including *MYC*, C is the *PVT1* region, and D is the region of telomeric to *PVT1*. *, frequency shows the case number for each of the breakpoint regions.

lymphoma cell line, Daudi, were analyzed. Each assay was done in triplicate.

Results

Frequent involvement of *PVT1* locus in 8q24 rearrangements

The 8q24 rearrangements were detected using 3 FISH probe sets in 12 patients (22.2%) and 8 cell lines (72.7%). The breakpoints of 8q24 were assigned to a 360 kb segment containing the *MYC* and *PVT1* genes in 10 patients with multiple myeloma and in all multiple myeloma cell lines, and 11 breakpoint types were identified (Fig. 1, Supplementary Fig. S1 and Supplementary Table S1). Breakpoint regions at 8q24 could be divided into 4 regions: approximately 120 kb centromeric to *MYC* (5′ side of *MYC*; region A), the region centromerically adjacent to *PVT1* (approximately 170 kb region, including *MYC*, of 5′ side of *PVT1*; region B), the *PVT1* region (region C), and the telomeric region to *PVT1* (3′ side of *PVT1*; region D; Fig. 1). In patients with multiple myeloma, region C was the most frequent (Fig. 1B), with breakpoints detected within the *PVT1* gene in 5 patients (41.7%; Pt-1 to 4, and 7). Region B was identified in 4 patients (33.3%; Pt- 7 to 10), and both regions A and C in 2 patients (16.7%; Pt- 5 and 6). The remaining 2 patients (16.7%; Pt- 11 and 12) showed breakpoints outside of these 3 regions (region D). Among the 8 cell lines with 8q24 rearrangements, breakpoints were identified in the *PVT1* (region C) in 3 cell lines (37.5%; AMU-MM1, LP-1, and KMS-34), in region B in 1 cell line (12.5%; AMO1), and in both regions A and C in 2 cell lines (25.0%; RPMI8226 and KMS-18). The breakpoints observed in KMS-28-PE and NCI-H929 were either centromeric or telomeric to *MYC* and *PVT1*. The SNP array analysis validated the interphase FISH data by showing copy number gains at the regions of interest in KMS-18, RPMI8226, and KMS-28-PE (Supplementary Fig. S2). In summary, breakpoints were assigned to the *PVT1* gene in 7 of 54 patients (13.0%) and 5 of 11 cell lines (45.5%), and to the *MYC* gene in 4 patients (7.4%) and 1 cell line (9.1%).

Partners of 8q24 rearrangement detected by SKY–FISH and genome copy number analysis

Metaphase analysis of 2 patients (Pt- 1 and 8) and 8 multiple myeloma cell lines by SKY, SKY–FISH, and FISH identified various translocation/insertion partner loci for 8q24 rearrangements (Fig. 2A and B and Supplementary Fig. S3). To detect the candidate genes within partner loci of 8q24 rearrangement, the boundaries of copy number gains and losses in the regions of interest were mapped using the SNP arrays (Table 1 and

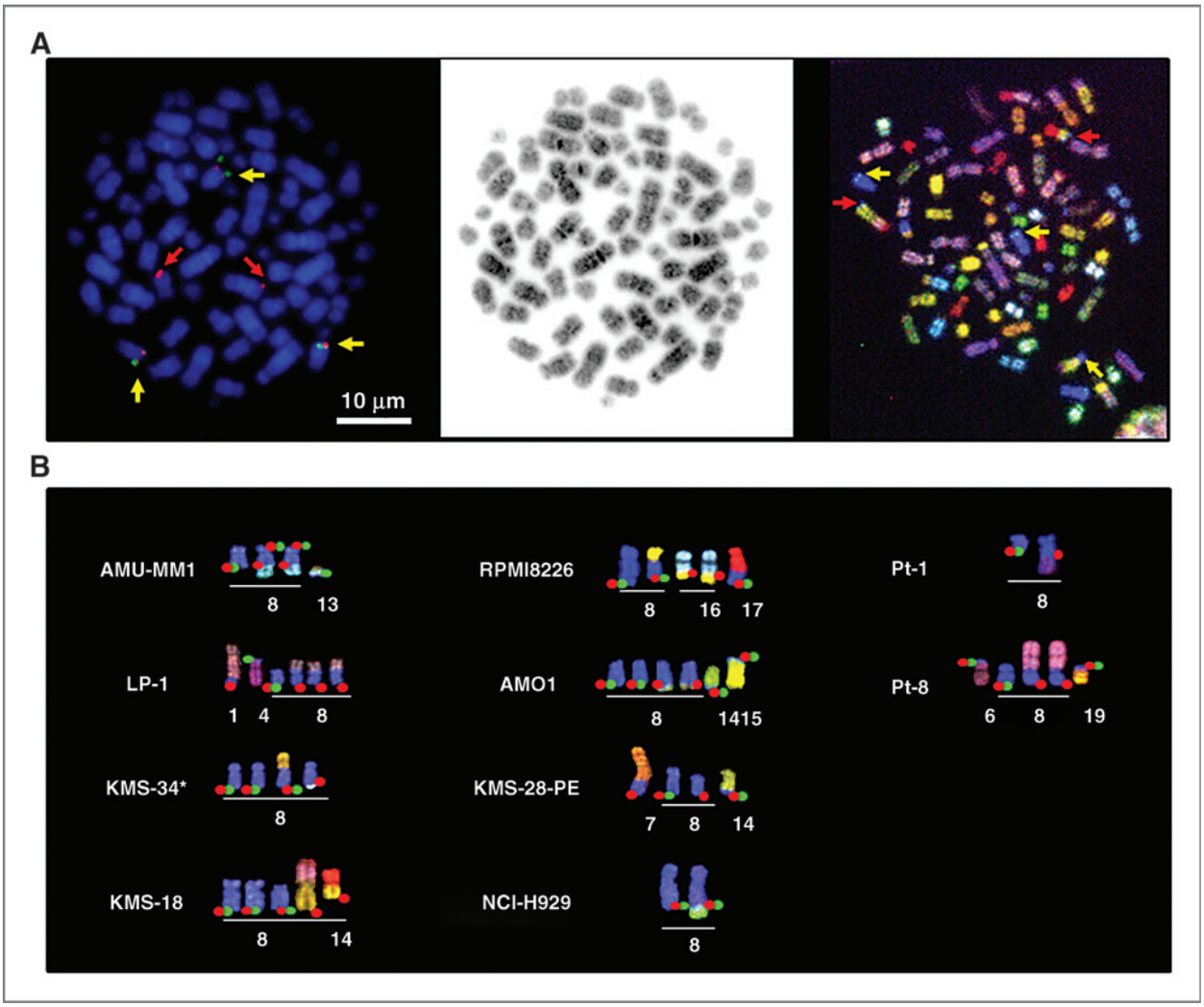

Figure 2. Detection of partner loci of 8q24 rearrangements by metaphase analysis. A, metaphase FISH with PVT1-A probe (left), inverted 4′, 6-diamidino-2-phenylindole (DAPI) staining (middle), and SKY–FISH (right) analysis of KMS-18. Red signals from the PVT1-A probe were detected on chromosome 14 by SKY–FISH (red arrows). Yellow arrows indicate fusion signals of red and green signals. Scale bar, 10 μm. B, partial karyotype of 8q24 rearrangement-positive samples using SKY–FISH. Red and green signals derived from the 8q24 (KMS-28-PE) or PVT1-A probes (other cell lines and clinical samples) are shown on each chromosome. Partial karyotype shows t(8;13)(q24;q13) in AMU-MM1, t(4;8)(p16;q24) in LP-1, t(8;16)(q24;q23-24) in KMS-34, t(8;14)(q24;q32) in KMS-18, der(16)t(16;22)ins(16;8)(q23;q24) in RPMI8226, t(8;14)(q24;q32) and t(8;15)(q24;?) in AMO1, t(8;14)(q24;q32) in KMS-28-PE, t(8;20)(q24;q11) in NCI-H929, t(4;8)(q?;q24) in Pt-1, and t(6;8)(p25;q24), and t(8;19)(q24;p13) in Pt-8. *, in KMS-34, interphase FISH signal pattern was YYYRR (Supplementary Table S1), however, one of the red signals could not be detected in SKY–FISH analysis because of few metaphases in KMS-34.

Supplementary Fig. S4). Chromosomal breakpoints, partner genes, and 8q24 rearrangement patterns identified 5 partner loci of *PVT1* translocations or insertions, 4p16, 4q13, 13q13, 14q32, and 16q23-24, in 5 of 8 cell lines and 1 of 2 primary multiple myeloma cells (Table 1).

Identification of the *PVT1-NBEA* and *PVT1-WWOX* chimeric genes in multiple myeloma cell lines

In AMU-MM1 cell line, the SKY analysis identified the unbalanced chromosomal translocation t(8;13)(q24;q13), which resulted in 2 der(8) and 1 der(13) (Fig. 3A). The SNP array analysis clearly showed that the copy number change at 8q24 occurred within the region including *PVT1* exon 1 and intron 1 (between the physical positions of 128871130 and 128909458, Fig. 3B). At 13q13, the copy number change occurred within intron 2 of *NBEA* (between the physical positions of 34477756 and 34734115, Fig. 3B). On the basis of these results, RT-PCR analysis was conducted to detect chimeric products using primers P1S and N3A and N2S and P3A. Direct sequencing of the PCR products generated using primers P1S and N3A and N2S and P3A revealed the fusion of 5′-*PVT1* exon 1 with *NBEA* exon 3-3′, and that of 5′-*NBEA* exon 2 with *PVT1* exon 3-3′ (Fig. 3C–E). The primers N2S and P2A did not yield any PCR product, suggesting the splicing out of *PVT1* exon 2 (Fig. 3C and D). In RPMI8226 cell line, the SKY–FISH analysis identified der(16)t(16;22)ins(16;8)(q23;q24) [Fig. 3F]. The SNP array analysis clearly showed that the copy number change at 8q24 occurred within intron 1 of *PVT1* (between the

Table 1. Partners of 8q24 rearrangements and candidate genes

	8q24 Rearrangements		Translocation partners		
Patients and cell lines	**Involved genes**	**Type of alterations**	**Partner loci**	**Previously reported genes**	**Candidate genes**
AMU-MM1	*PVT1*	Translocation	13q13	*RB*	*NBEA*
LP-1	*PVT1*	Translocation	4p16	*FGFR3*, *MMSET*	*MMSET*
KMS-34	*PVT1*	Translocation	16q23-24	*WWOX*, *MAF*	—[a]
Pt-1	*PVT1*	Translocation	4q13	—[b]	*EPHA5*
RPMI8226	*PVT1*[c]	Insertion and gain	16q23	*WWOX*, *MAF*	*WWOX*
KMS-18	*PVT1*[c]	Translocation and gain	14q32	*IGH*	*ATG2B*
AMO1	*MYC*	Translocation	14q32, No.15	*IGH*, —[b]	*TRAF3/TDRD9*, *TUBGCP5*
Pt-8	*MYC*	Translocation	6p25, 19p13	*IRF4*, —[b]	*RNF8/FTSJD2*, *EFNA2/MUM1/GNG7*
KMS-28-PE	Unknown	Translocation and gain	14q32	*IGH*	—[a]
NCI-H929	Unknown	Translocation	20q11	*MAFB*	NA

Abbreviation: NA, not available.

[a]No copy number change was found at chromosome 16 in KMS-34. The rearranged gene could not be identified, because there were too many genes within the region in which copy number change occurred in KMS-28-PE (Supplementary Fig. S4).

[b]No gene has been reported as affected in multiple myeloma.

[c]Duplication of both the *MYC* locus and centromeric part of *PVT1* was detected in RPMI8226 and KMS-18 with *PVT1* rearrangement.

physical position of 128,891,891 and 128,902,659, Fig. 3G). At 16q23, the copy number change occurred within intron 8 of *WWOX* (between the physical position of 77,399,684 and 77,401,485, Fig. 3G). On the basis of these results, RT-PCR analysis was conducted to detect chimeric products using primers P1S and W9A (Fig. 3H), and direct sequencing of this product revealed the fusion of 5′-*PVT1* exon 1 with *WWOX* exon 9-3′ (Fig. 3I and J). However, these chimeric transcripts were not detected in 7 patients with *PVT1* rearrangements.

The expression level of *PVT1-NBEA* and *PVT1-WWOX* transcripts was measured by real-time quantitative RT-PCR (RQ-PCR; Fig. 4A and B). High expression of aberrant *NBEA* was detected in AMU-MM1 cell line using the NBEA 58-59 primer probe set. In contrast, no expression of normal *NBEA* was detected using the NBEA 2-3 primer probe set in AMU-MM1, whereas normal *NBEA* was detected in all other cell lines in which it was expressed at similar levels. These results indicate that the 5′-*PVT1-NBEA*-3′ chimeric transcript is highly expressed in AMU-MM1 cells. Similarly, expression of *WWOX* exon 9 was higher than *WWOX* exon 8-9 in RPMI8226, suggesting that a part of expression of exon 9 was due to *PVT1-WWOX* chimeric transcript.

Discussion

The present study uncovered 2 aspects of molecular genetics in multiple myeloma. The first finding is the frequent rearrangement of *PVT1* gene in multiple myeloma harboring 8q24 rearrangements. *PVT1* is the human homolog of the mouse *Pvt1* oncogene, which was originally identified as a common retroviral integration site in murine leukemia virus (MLV)–induced T lymphomas. *PVT1/Pvt1* is also involved in variants t(2;8), t(8;22), or t(8;14) in human Burkitt lymphoma and in variant t(6;15) in mouse plasmacytomas (10, 15, 22–25). Moreover, amplification of the *PVT1* gene has been observed in several cancers including lymphomas (26–30), and *PVT1* overexpression was found to contribute to the suppression of apoptosis (31). The *PVT1* locus is thought to encode several miRNAs important in oncogenesis (32). Hence, the current study suggests that *PVT1* is one of the target genes of rearrangement that may be responsible for driving multiple myeloma, whereas other studies have shown breakpoints within the region centromeric to *PVT1* (9–11, 33).

The second finding is the novel chimeric genes, *PVT1-NBEA* and *PVT1-WWOX*, in the multiple myeloma cell lines, the AMU-MM1 cell line with t(8;13)(q24;q13), and RPMI8226 cell line with der(16)t(16;22)ins(16;8)(q23;q24), resulting in high expression of the abnormal chimeric transcript. In *PVT1-NBEA*, the breakpoint of *PVT1* was found within intron 1 and *PVT1* exon 1 was found to be fused to *NBEA* exon 3, resulting in the loss of the start codon in *NBEA* exon 2. In this setting, the second ATG in exon 3 of the *NBEA* gene may function as a start codon to produce a putative abnormal NBEA protein lacking 107 N-terminal amino acids (Fig. 3E), although the expression of *PVT1-NBEA* at the protein level remains to be investigated. Although, knockdown of *PVT1-NBEA* using siRNA could not inhibit proliferation and induces cell death (Supplementary Fig. S5), it would be important to investigate the function of this *NBEA* chimera in multiple myeloma tumorigenesis, as NBEA modulates signal transduction and vesicular trafficking

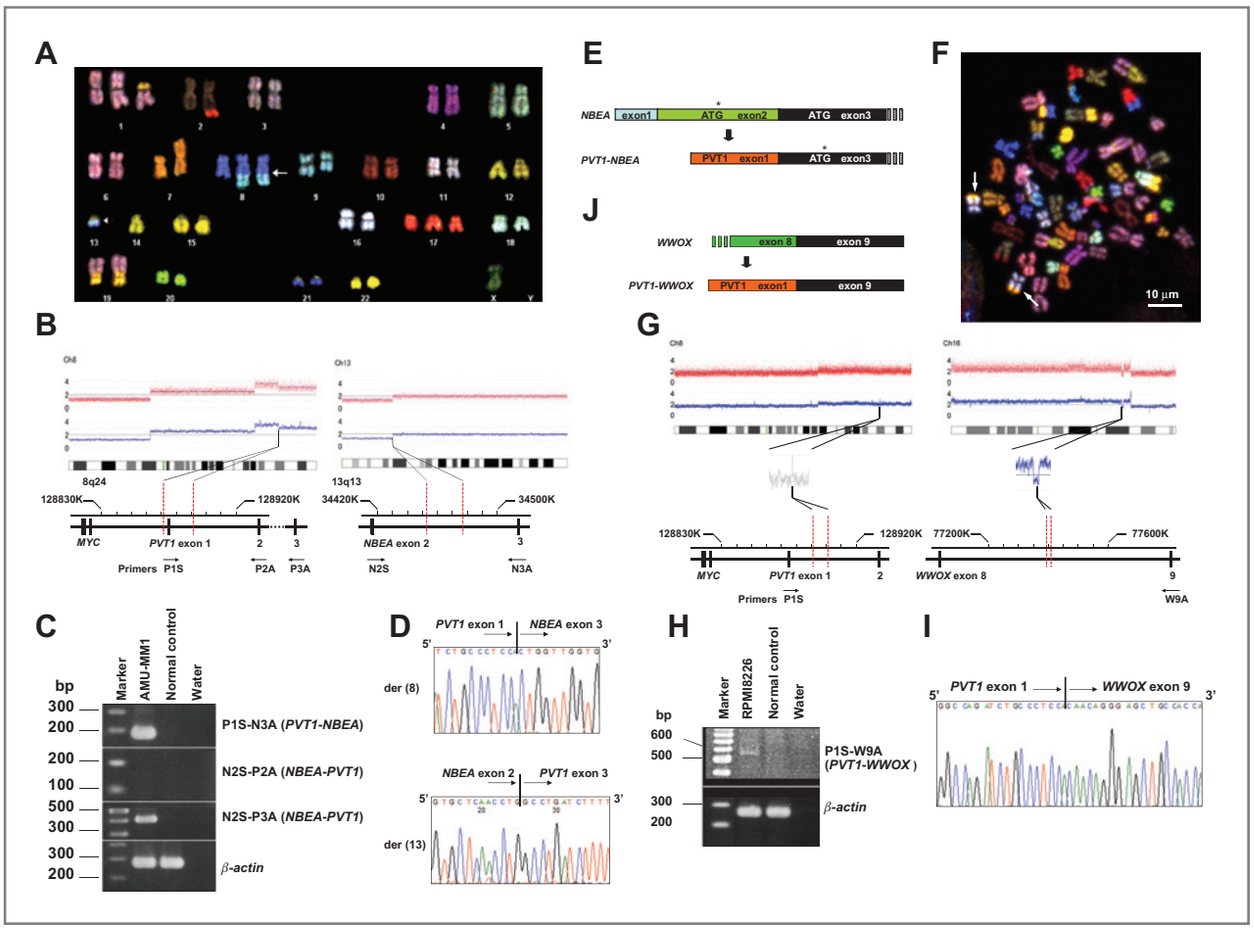

Figure 3. Identification of *PVT1-NBEA* and *PVT1-WWOX* chimeric genes in multiple myeloma cell lines. A, SKY analysis of AMU-MM1 reveals a complex karyotype including t(8;13)(q24;q13) as 46,X,-X,+der(1;19)(q10;p10),der(2)t(2;17)(q37;q11.2),der(7)(qter → q11.2::p15 → q11.2::7?), t(8;13)(q24;q13),+der(8)t(8;13),del(12)(p11.2),-13,der(19)t(1;19)(q12;p13)×2,del(20)(p13). Arrow, breakpoint of der(8)t(8;13)(q24;q13); arrowhead, breakpoint of der(13)t(8;13)(q24;q13). B, copy number changes at 8q24 (*PVT1*) and 13q13 (*NBEA*) detected by SNP array. Primers used to detect chimeric transcript. The *y*-axes indicate the linear scale corresponding to genome copy number of each chromosome. However, copy number data have never been corrected for the influence of tumor cell percentage or real copy number of some chromosomes. C, detection of *PVT1-NBEA* and *NBEA-PVT1* chimeric transcripts by RT-PCR. D, sequencing of chimeric junction of *PVT1-NBEA* and *NBEA-PVT1* chimeric transcripts. E, putative structure of abnormal *NBEA* fusion transcript. *PVT1-NBEA* lacks a start codon in *NBEA* exon 2; the second ATG in exon 3 might function as a start codon, resulting in an abnormal NBEA protein lacking its N-terminus. *, ATG indicates start codon. F, SKY–FISH analysis of RPMI8226 reveals a complex karyotype including der(16)t(16;22)ins(16;8)(q23;q24). Arrows indicate red signals of PVT1-A inserting to t(16;22). It is difficult to detect the 8q24 locus on der(16) using conventional cytogenetic technique. Scale bar, 10 μm. G, copy number changes at 8q24 (*PVT1*) and 16q23 (*WWOX*) detected by SNP array. Primers used to detect chimeric transcript. The *y*-axes indicate genome copy number. H, detection of *PVT1-WWOX* chimeric transcript by RT-PCR. I, sequencing of chimeric junction of *PVT1-WWOX* chimeric transcript. J, putative structure of abnormal *WWOX* fusion transcript.

in neurons and other cells, and as gene abnormality and aberrant expression of *NBEA* have been associated with plasma cell dyscrasias (34–36). In addition, the association between the *PVT1-NBEA* fusion gene and the t(8;13) chromosomal abnormality, which has been reported in a small population of multiple myeloma, remains to be verified (7, 11, 37, 38). Chromosome 13 is often deleted in multiple myeloma and this has been linked to poorer prognosis. In such cases with loss of chromosome 13, *RB1* is thought to be a major target and driver. However, a group has reported *NBEA* to also be a target of recurrent interstitial deletions at 13q13 and proposed that *NBEA* might be a tumor suppressor gene in multiple myeloma (36). *WWOX* is generally considered to be a candidate tumor suppressor gene, and known to have a proapoptotic effect by participating in the TNF apoptotic pathway and via direct physical interaction with p53 and its homolog p73 (39). However, immunohistochemistry revealed that WWOX protein levels were rather elevated in gastric and breast carcinoma (40). Therefore, *WWOX* did not seem to act as tumor suppressor gene simply. Interestingly, although both *NBEA* and *WWOX* are located at common fragile site, usually contributing to gene inactivation, FRA13A and FRA16D, respectively, these genes highly express via fusion to *PVT1* (41, 42). It would be important to further elucidate the function of *NBEA* and *WWOX*. Several translocation/insertion partners of 8q24 rearrangements were identified in the remaining samples (Table 1). The genes

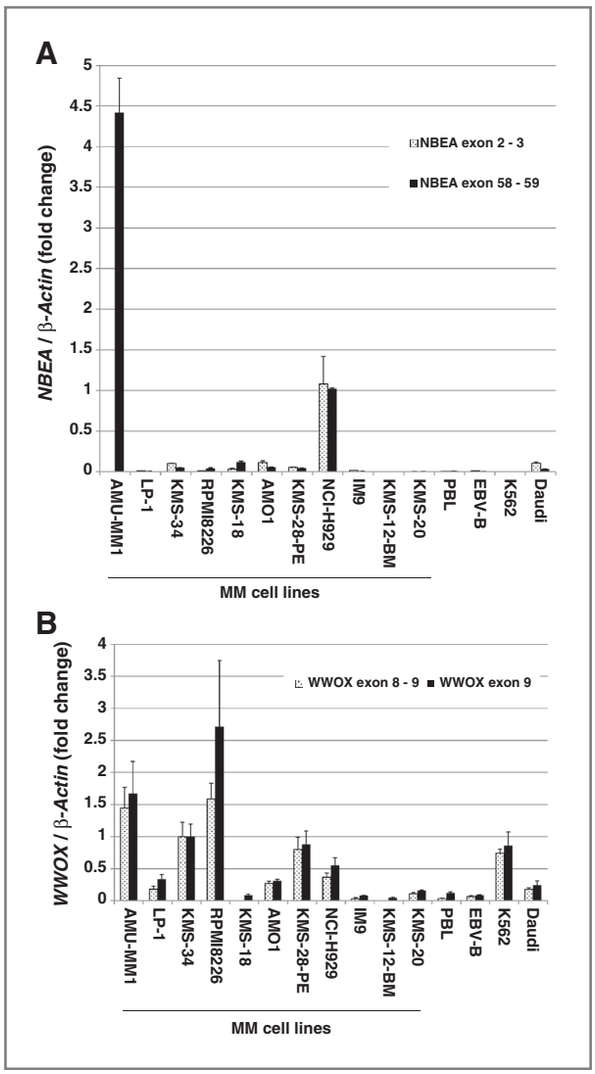

Figure 4. Expression of *NBEA* and *WWOX* in cell lines. A, RQ-PCR analysis showing that the abnormal *NBEA* transcript is highly expressed in the AMU-MM1 cell line as compared with other multiple myeloma cell lines, normal lymphocytes, an Epstein–Barr virus–transformed B-cell line, a leukemia cell line (K562), and a Burkitt lymphoma cell line (Daudi). Dotted and black bars indicate expression levels using the NBEA 2-3 and NBEA 58-59 primer sets, respectively. B, RQ-PCR analysis showing that the abnormal *WWOX* transcript is relatively highly expressed in the RPMI8226 cell line as compared with other cell lines. Dotted and black bars indicate expression levels using the WWOX 8-9 and WWOX 9 primer sets, respectively.

located at translocation/insertion breakpoints, identified by copy number analysis, have been frequently associated with cancer (43–49). No chimeric genes could be cloned in other samples. In Pt-1, LP-1, and KMS-18, *PVT1* was translocated to the regions of *EPHA5*, *MMSET*, or *ATG2B* with opposite direction of transcription, suggesting that these genes are not involved in the fusion with *PVT1*. In KMS-34, AMO1, Pt-8, KMS-28PE, and NCI-H929, genome copy number changes were not identified within a single gene at 8q24 and/or partner loci (Supplementary Fig. S4). The translocation/insertion partner breakpoints identified in the present study warrant further molecular analysis of the candidate genes.

The relationship between *MYC* and *PVT1* in terms of multiple myeloma development and progression is difficult to elucidate. RQ-PCR analysis revealed high expression of *PVT1* and *MYC* in most multiple myeloma cell lines regardless of *PVT1* or *MYC* rearrangement status (Supplementary Fig. S6). Results showed that 8q24 rearrangements included various complex translocations with either deletion or insertion of a part of the 8q24 segment including *MYC* and the centromeric segment of *PVT1*. In addition, gains of chromosome 8, including *PVT1* and *MYC*, are frequently identified in multiple myeloma cell lines (Fig 1B, Supplementary Fig. S1B). These gains are likely to contribute to the amplification of the *PVT1* and *MYC* genes (28). Beyond chromosomal abnormalities, the molecular mechanisms underlying *MYC* overexpression in multiple myeloma, such as interaction with *PVT1* or deregulation of miRNAs, warrant further research (32, 50).

In conclusion, *PVT1* is frequently involved with various partner loci in multiple myeloma with 8q24 abnormalities, and, *PVT1-NBEA* and *PVT1-WWOX* were identified as novel, highly expressed chimeric genes in which *NBEA* and *WWOX* are fused with *PVT1* in multiple myeloma cell lines harboring t(8;13)(q24;q13) and der(16)t(16;22)ins(16;8)(q23;q24), respectively. These findings suggest that *PVT1* rearrangements may represent a novel molecular paradigm underlying the pathology of multiple myeloma with 8q24 rearrangements.

Disclosure of Potential Conflicts of Interest

No potential conflicts of interest were disclosed.

Authors' Contributions

Conception and design: I. Hanamura, K. Nishida, J. Kuroda, M. Taniwaki
Development of methodology: H. Nagoshi, T. Otsuki, K. Nishida, S. Horiike
Acquisition of data (provided animals, acquired and managed patients, provided facilities, etc.): K. Nishida, S. Horiike, J. Kuroda
Analysis and interpretation of data (e.g., statistical analysis, biostatistics, computational analysis): H. Nagoshi, T. Taki, I. Hanamura, K. Nishida, K. Okuda, N. Sakamoto, S. Kobayashi, M. Yamamoto-Sugitani, Y. Tsutsumi, T. Kobayashi, Y. Matsumoto, S. Horiike, J. Kuroda, M. Taniwaki
Writing, review, and/or revision of the manuscript: H. Nagoshi, T. Taki, I. Hanamura, K. Nishida, S. Horiike, J. Kuroda, M. Taniwaki
Administrative, technical, or material support (i.e., reporting or organizing data, constructing databases): H. Nagoshi, T. Taki, I. Hanamura, K. Nishida, S. Horiike
Study supervision: T. Taki, M. Nitta, K. Nishida, S. Horiike, J. Kuroda, M. Taniwaki

Acknowledgments

The authors thank Kayoko Kurita and Akari Kazami for their expert technical assistance.

Grant Support

This work was supported by a Grant-in-Aid for Cancer Research from the Ministry of Health, Labor and Welfare of Japan, by a Grant-in-aid for Scientific Research (B) and (C) from the Ministry of Education, Culture, Sports, Science and Technology of Japan, and by the National Cancer Center Research and Development Fund.

The costs of publication of this article were defrayed in part by the payment of page charges. This article must therefore be hereby marked *advertisement* in accordance with 18 U.S.C. Section 1734 solely to indicate this fact.

Received January 24, 2012; revised May 29, 2012; accepted June 18, 2012; published OnlineFirst August 6, 2012.

References

1. Fonseca R, Bergsagel PL, Drach J, Shaughnessy J, Gutierrez N, Stewart AK, et al. International Myeloma Working Group. International Myeloma Working Group molecular classification of multiple myeloma: spotlight review. Leukemia 2009;23:2210–21.
2. Chen KC, Bevan PC, Matthews JG. Analysis of G banded karyotypes in myeloma cells. J Clin Pathol 1986;39:260–6.
3. Hanamura I, Stewart JP, Huang Y, Zhan F, Santra M, Sawyer JR, et al. Frequent gain of chromosome band 1q21 in plasma-cell dyscrasias detected by fluorescence *in situ* hybridization: incidence increases from MGUS to relapsed myeloma and is related to prognosis and disease progression following tandem stem-cell transplantation. Blood 2006;108:1724–32.
4. Gould J, Alexanian R, Goodacre A, Pathak S, Hecht B, Barlogie B. Plasma cell karyotype in multiple myeloma. Blood 1988;71:453–6.
5. Sawyer JR, Waldron JA, Jagannath S, Barlogie B. Cytogenetic findings in 200 patients with multiple myeloma. Cancer Genet Cytogenet 1995;82:41–9.
6. Nishida K, Tamura A, Nakazawa N, Ueda Y, Abe T, Matsuda F, et al. The Ig heavy chain gene is frequently involved in chromosomal translocations in multiple myeloma and plasma cell leukemia as detected by *in situ* hybridization. Blood 1997;90:526–34.
7. Avet-Loiseau H, Gerson F, Magrangeas F, Minvielle S, Harousseau JL, Bataille R, et al. Intergroupe Francophone du Myélome.Rearrangements of the c-myc oncogene are present in 15% of primary human multiple myeloma tumors. Blood 2001;98:3082–6.
8. Sawyer JR, Lukacs JL, Thomas EL, Swanson CM, Goosen LS, Sammartino G, et al. Multicolour spectral karyotyping identifies new translocations and a recurring pathway for chromosome loss in multiple myeloma. Br J Haematol 2001;112:167–74.
9. Fabris S, Storlazzi CT, Baldini L, Nobili L, Lombardi L, Maiolo AT, et al. Heterogeneous pattern of chromosomal breakpoints involving the MYC locus in multiple myeloma. Genes Chromosomes Cancer 2003;37:261–9.
10. Shou Y, Martelli ML, Gabrea A, Qi Y, Brents LA, Roschke A, et al. Diverse karyotypic abnormalities of the c-myc locus associated with c-myc dysregulation and tumor progression in multiple myeloma. Proc Natl Acad Sci U S A 2000;97:228–33.
11. Dib A, Gabrea A, Glebov OK, Bergsagel PL, Kuehl WM. Characterization of MYC translocations in multiple myeloma cell lines. J Natl Cancer Inst Monogr 2008;39:25–31.
12. Avet-Loiseau H, Daviet A, Brigaudeau C, Callet-Bauchu E, Terré C, Lafage-Pochitaloff M, et al. Cytogenetic, interphase, and multicolor fluorescence *in situ* hybridization analyses in primary plasma cell leukemia: a study of 40 patients at diagnosis, on behalf of the Intergroupe Francophone du Myélome and the Groupe Français de Cytogénétique Hématologique. Blood 2001; 97:822–5.
13. Mohamed AN, Bentley G, Bonnett ML, Zonder J, Al-Katib A. Chromosome aberrations in a series of 120 multiple myeloma cases with abnormal karyotypes. Am J Hematol 2007;82:1080–7.
14. Shiramizu B, Magrath I. Localization of breakpoints by polymerase chain reactions in Burkitt's lymphoma with 8;14 translocations. Blood 1990;75:1848–52.
15. Shtivelman E, Bishop JM. Effects of translocations on transcription from PVT. Mol Cell Biol 1990;10:1835–9.
16. Hanamura I, Goto M, Nagoshi H, Taki T, Imai N, Suganuma K, et al. Establishment and characterization of a novel human myeloma cell line, AMU-MM1, from a multiple myeloma patient involving central nerve system after treatment with bortezomib. Blood 2010;116: (abstract [4991]).
17. Taniwaki M, Sliverman GA, Nishida K, Horiike S, Misawa S, Shimazaki C, et al. Translocations and amplification of the BCL2 gene are detected in interphase nuclei of non-Hodgkin's lymphoma by *in situ* hybridization with yeast artificial chromosome clones. Blood 1995;86: 1481–6.
18. Kakazu N, Taniwaki M, Horiike S, Nishida K, Tatekawa T, Nagai M, et al. Combined spectral karyotyping and DAPI banding analysis of chromosome abnormalities in myelodysplastic syndrome. Genes Chromosomes Cancer 1999;26:336–45.
19. Shaffer LG, Slovak ML, Campbell LJ, editors. ISCN: an international system of human cytogenetic nomenclature. Basel, Switzerland: Karger; 2009.
20. Nannya Y, Sanada M, Nakazaki K, Hosoya N, Wang L, Hangaishi A, et al. A robust algorithm for copy number detection using high-density oligonucleotide single nucleotide polymorphism genotyping arrays. Cancer Res 2005;65:6071–9.
21. Chinen Y, Taki T, Nishida K, Shimizu D, Okuda T, Yoshida N, et al. Identification of the novel AML1 fusion partner gene, LAF4, a fusion partner of MLL, in childhood T-cell acute lymphoblastic leukemia with t (2;21)(q11;q22) by bubble PCR method for cDNA. Oncogene 2008;27: 2249–56.
22. Henglein B, Synovzik H, Groitl P, Bornkamm GW, Hartl P, Lipp M. Three breakpoints of variant t(2;8) translocations in Burkitt's lymphoma cells fall within a region 140 kilobases distal from c-myc. Mol Cell Biol 1989;9:2105–13.
23. Rack KA, Delabesse E, Radford-Weiss I, Bourquelot P, Le Guyader G, Vekemans M, et al. Simultaneous detection of MYC, BVR1, and PVT1 translocations in lymphoid malignancies by fluorescence *in situ* hybridization. Genes Chromosomes Cancer 1998;23:220–6.
24. Villeneuve L, Rassart E, Jolicoeur P, Graham M, Adams JM. Proviral integration site Mis-1 in rat thymomas corresponds to the pvt-1 translocation breakpoint in murine plasmacytomas. Mol Cell Biol 1986;6:1834–7.
25. Huppi K, Siwarski D. Chimeric transcripts with an open reading frame are generated as a result of translocation to the Pvt-1 region in mouse B-cell tumors. Int J Cancer 1994;59:848–51.
26. Asker C, Mareni C, Coviello D, Ingvarsson S, Sessarego M, Origone P, et al. Amplification of c-myc and pvt-1 homologous sequences in acute nonlymphatic leukemia. Leuk Res 1988;12:523–7.
27. Shtivelman E, Bishop JM. The PVT gene frequently amplifies with MYC in tumor cells. Mol Cell Biol 1989;9:1148–54.
28. Bakkus MH, Brakel-van Peer KM, Michiels JJ, van't Veer MB, Benner R. Amplification of the c-myc and the pvt-like region in human multiple myeloma. Oncogene 1990;5:1359–64.
29. Costinean S, Zanesi N, Pekarsky Y, Tili E, Volinia S, Heerema N, et al. Pre-B cell proliferation and lymphoblastic leukemia/high-grade lymphoma in E(mu)-miR155 transgenic mice. Proc Natl Acad Sci U S A 2006;103:7024–9.
30. Carramusa L, Contino F, Ferro A, Minafra L, Perconti G, Giallongo A, et al. The PVT-1 oncogene is a Myc protein target that is overexpressed in transformed cells. J Cell Physiol 2007;213:511–8.
31. Guan Y, Kuo WL, Stilwell JL, Takano H, Lapuk AV, Fridlyand J, et al. Amplification of PVT1 contributes to the pathophysiology of ovarian and breast cancer. Clin Cancer Res 2007;13:5745–55.
32. Huppi K, Volfovsky N, Runfola T, Jones TL, Mackiewicz M, Martin SE, et al. The identification of microRNAs in a genomically unstable region of human chromosome 8q24. Mol Cancer Res 2008;6: 212–21.
33. Palumbo AP, Boccadoro M, Battaglio S, Corradini P, Tsichlis PN, Huebner K, et al. Human homologue of Moloney leukemia virus integration-4 locus (MLVI-4), located 20 kilobases 3′ of the myc gene, is rearranged in multiple myelomas. Cancer Res 1990;50: 6478–82.
34. Wang X, Herberg FW, Laue MM, Wullner C, Hu B, Petrasch-Parwez E, et al. Neurobeachin: a protein kinase A-anchoring, beige/Chediak-higashi protein homolog implicated in neuronal membrane traffic. J Neurosci 2000;20:8551–65.
35. Zhan F, Barlogie B, Arzoumanian V, Huang Y, Williams DR, Hollmig K, et al. Gene-expression signature of benign monoclonal gammopathy evident in multiple myeloma is linked to good prognosis. Blood 2007;109:1692–700.
36. O'Neal J, Gao F, Hassan A, Monahan R, Barrios S, Kilimann MW, et al. Neurobeachin (NBEA) is a target of recurrent interstitial deletions at 13q13 in patients with MGUS and multiple myeloma. Exp Hematol 2009;37:234–44.
37. Sáez B, Martín-Subero JI, Largo C, Martín MC, Odero MD, Prosper F, et al. Identification of recurrent chromosomal breakpoints in multiple myeloma with complex karyotypes by combined G-banding, spectral

karyotyping, and fluorescence *in situ* hybridization analyses. Cancer Genet Cytogenet 2006;169:143–9.
38. Chiecchio L, Dagrada GP, Protheroe RK, Stockley DM, Smith AG, Orchard KH, et al. UK Myeloma Forum. Loss of 1p and rearrangement of MYC are associated with progression of smouldering myeloma to myeloma: sequential analysis of a single case. Haematologica 2009;94:1024–8.
39. Aqeilan RI, Pekarsky Y, Herrero JJ, Palamarchuk A, Letofsky J, Druck T, et al. Functional association between Wwox tumor suppressor protein and p73, a p53 homolog. Proc Natl Acad Sci U S A 2004;101:4401–6.
40. Watanabe A, Hippo Y, Taniguchi H, Iwanari H, Yashiro M, Hirakawa K, et al. An opposing view on WWOX protein function as a tumor suppressor. Cancer Res 2003;63:8629–33.
41. Savelyeva L, Sagulenko E, Schmitt JG, Schwab M. The neurobeachin gene spans the common fragile site FRA13A. Hum Genet 2006;118:551–8.
42. Bednarek AK, Laflin KJ, Daniel RL, Liao Q, Hawkins KA, Aldaz CM. WWOX, a novel WW domain-containing protein mapping to human chromosome 16q23.3-24.1, a region frequently affected in breast cancer. Cancer Res 2000;60:2140–5.
43. Fu DY, Wang ZM, Wang BL, Chen L, Yang WT, Shen ZZ, et al. Frequent epigenetic inactivation of the receptor tyrosine kinase EphA5 by promoter methylation in human breast cancer. Hum Pathol 2010;41:48–58.
44. Annunziata CM, Davis RE, Demchenko Y, Bellamy W, Gabrea A, Zhan F, et al. Frequent engagement of the classical and alternative NF-kappaB pathways by diverse genetic abnormalities in multiple myeloma. Cancer Cell 2007;12:115–30.
45. Keats JJ, Fonseca R, Chesi M, Schop R, Baker A, Chng WJ, et al. Promiscuous mutations activate the noncanonical NF-kappaB pathway in multiple myeloma. Cancer Cell 2007;12:131–44.
46. Braggio E, Keats JJ, Leleu X, Van Wier S, Jimenez-Zepeda VH, Valdez R, et al. Identification of copy number abnormalities and inactivating mutations in two negative regulators of nuclear factorkappaB signaling pathways in Waldenstroms macroglobulinemia. Cancer Res 2009;69:3579–88.
47. Giefing M, Arnemann J, Martin-Subero JI, Nieländer I, Bug S, Hartmann S, et al. Identification of candidate tumour suppressor gene loci for Hodgkin and Reed–Sternberg cells by characterisation of homozygous deletions in classical Hodgkin lymphoma cell lines. Br J Haematol 2008;142:916–24.
48. Ohta M, Mimori K, Fukuyoshi Y, Kita Y, Motoyama K, Yamashita K, et al. Clinical significance of the reduced expression of G protein gamma 7 (GNG7) in oesophageal cancer. Br J Cancer 2008;98:410–7.
49. Shibata K, Mori M, Tanaka S, Kitano S, Akiyoshi T. Identification and cloning of human G-protein gamma 7, down-regulated in pancreatic cancer. Biochem Biophys Res Commun 1998;246:205–9.
50. Sasaki N, Kuroda J, Nagoshi H, Yamamoto M, Kobayashi S, Tsutsumi Y, et al. Bcl-2 is a better therapeutic target than c-Myc, but attacking both could be a more effective treatment strategy for B-cell lymphoma with concurrent Bcl-2 and c-Myc overexpression. Exp Hematol 2011;39:817–28.